

## SYNTHESIS AND STRUCTURAL CHARACTERIZATION OF STRONTIUM CONTAINING BIOACTIVE GLASSES

MARIA STEINER<sup>a</sup>, ROZALIA VERES<sup>a,\*</sup>, VIORICA SIMON<sup>a</sup>

**ABSTRACT.** Bioactive glasses of SiO<sub>2</sub>-CaO-SrO-P<sub>2</sub>O<sub>5</sub> system, wherein SrO progressively replaced up to 4 mol% CaO, were produced using the sol-gel route. Their structural properties and bioactivity were tested using differential thermal analysis (DTA), X-ray diffraction (XRD) and Fourier transform infrared spectroscopy (FT-IR). Based on the DTA results, the 110 °C dried gels were subjected to heat treatment at 600 °C. X-ray diffractograms show a predominant amorphous character for all samples. FT-IR results indicate few changes in the local structure by progressive addition of strontium. The soaking of samples for 14 days in biological fluid resulted in the formation of hydroxyapatite layer that delivered characteristic infrared absorption band sensitive to strontium content.

**Keywords:** *bioactive glasses; sol-gel; strontium; in vitro bioactivity.*

### INTRODUCTION

Osteoporosis is a skeletal disorder characterized by compromised bone strength predisposing to an increased risk of fracture [1]. In osteoporotic bone, osteoclasts resorb too much bone, while osteoblastic bone formation is not sufficient to counterbalance this, resulting in reduced bone mineral density, weak and brittle bones [2].

Therefore, in last decades there has been large amount of work on developing synthetic materials for bone regeneration and replacing. Bioactive glasses are a group of synthetic materials with bone bonding properties first discovered by Hench [3, 4]. They have the ability of direct bonding to bone via formation of a surface carbonated hydroxyapatite layer when exposed to simulated body fluid (SBF) [5, 6]. Many bioactive glass compositions including copper [7], silver [8] magnesium [9], zinc [10, 11] and strontium as dopants have been studied and have shown considerable efficacy in bone regeneration [12-15].

---

<sup>a</sup> Babeş-Bolyai University, Faculty of Physics & Institute of Interdisciplinary Research in Bio-Nano-Sciences, Cluj-Napoca RO-400084, Romania

\* Corresponding author: rozalia.veres@ubbcluj.ro

It was reported that the introduction of strontium ions into silicate matrix leads to bone formation and inhibites bone resorption by osteoclasts, promoting the increase of bone density and resistance [16, 17]. The advantages of strontium-doped bioactive glasses are based on the controlled release of the Sr ions that stimulate the activity of osteoblast cells. Strontium can substitute for calcium in bioactive glasses, and this replacement may induce few structural changes [14] that influence the gradual degradation of the bioactive material, with effects on new bone formation on the implant surface [18, 19].

The objective of the present study was to produce new sol-gel derived bioactive glasses of  $\text{SiO}_2\text{-CaO-SrO-P}_2\text{O}_5$  system and to characterize their structural properties and bioactivity.

## RESULTS AND DISCUSSION

In the investigated  $65\text{SiO}_2\text{-}5\text{P}_2\text{O}_5\text{-(}30\text{-}x\text{)CaO}\cdot x\text{SrO}$  glass system ( $0\leq x\leq 4$  mol%) we explored five compositions, i.e.  $x = 0, 0.5, 1, 2$  and  $4$  mol%. The corresponding samples were noted Sr0, Sr0.5, Sr1, Sr2 and Sr4, respectively.

The TGA curves for all samples present several regions of weight loss (Figure 1). The first weight loss is associated with an endothermic peak in DTA curve that occurs around  $80^\circ\text{C}$  and can be ascribed to the loss of free water molecules. A second weight loss can be observed until  $400^\circ\text{C}$ . This loss can be associated with the elimination of water caged in pores and the decomposition of residual nitrates. The peaks observed around  $550^\circ\text{C}$  arise from dehydroxylation [20]. Based on these results, a thermal treatment at  $600^\circ\text{C}$  was considered.

The X-ray diffraction patterns for all samples treated at  $600^\circ\text{C}$  for 2 hours (Figure 2) indicate a predominant amorphous structure, without significant crystalline phases. The large diffraction peaks at about  $32^\circ$  might show a tendency to calcium strontium phosphate crystals (JCPDS 34-0484), excepting the sample without strontium oxide.

The structural properties of the glasses treated at  $600^\circ\text{C}$  were also analyzed through Fourier Transform Infrared Spectroscopy (FTIR). The absorption band recorded at  $3512\text{ cm}^{-1}$  (Figure 3) can be assigned to silanol groups linked to molecular water through hydrogen bonds and the band appeared at  $1648\text{ cm}^{-1}$  to the bending mode of adsorbed molecular water [21]. The bands occurring in the spectral region  $1560\text{-}1370\text{ cm}^{-1}$  correspond to carbonate species arising from the slight reaction between the glass samples and carbon dioxide from the atmosphere and might be also due to the formation of small quantities of calcium/strontium carbonates [22]. The broad band located in  $1300\text{-}800\text{ cm}^{-1}$  range is present in all the samples and is specific for silica-based bioactive glasses [23-24]. The shoulder at  $1234\text{ cm}^{-1}$  is attributed to

bending mode of Si–O–Si group. The peak observed at  $1062\text{ cm}^{-1}$  can be assigned to the Si–O–Si asymmetric stretching mode of bridging oxygen (BO), whereas the shoulder situated at  $939\text{ cm}^{-1}$  can be attributed to the Si–O asymmetric stretching mode of the non-bridging oxygen bonds (NBO) [25, 26]. A decrease of this signal intensity is noticed with the increase of SrO content. Withal, a shift of the absorption band assigned to Si–O–Si vibrations to lower wavenumbers is observed, suggesting the shortening of Si–O–Si bonds in the vicinity of large Sr cations [27, 28]. In all the investigated glasses is observed around  $551\text{ cm}^{-1}$  a band which corresponds to bending vibration of amorphous P–O bond [29]. Furthermore, the band situated in the range  $510\text{--}460\text{ cm}^{-1}$  can be ascribed to the Si–O–Si bending mode.

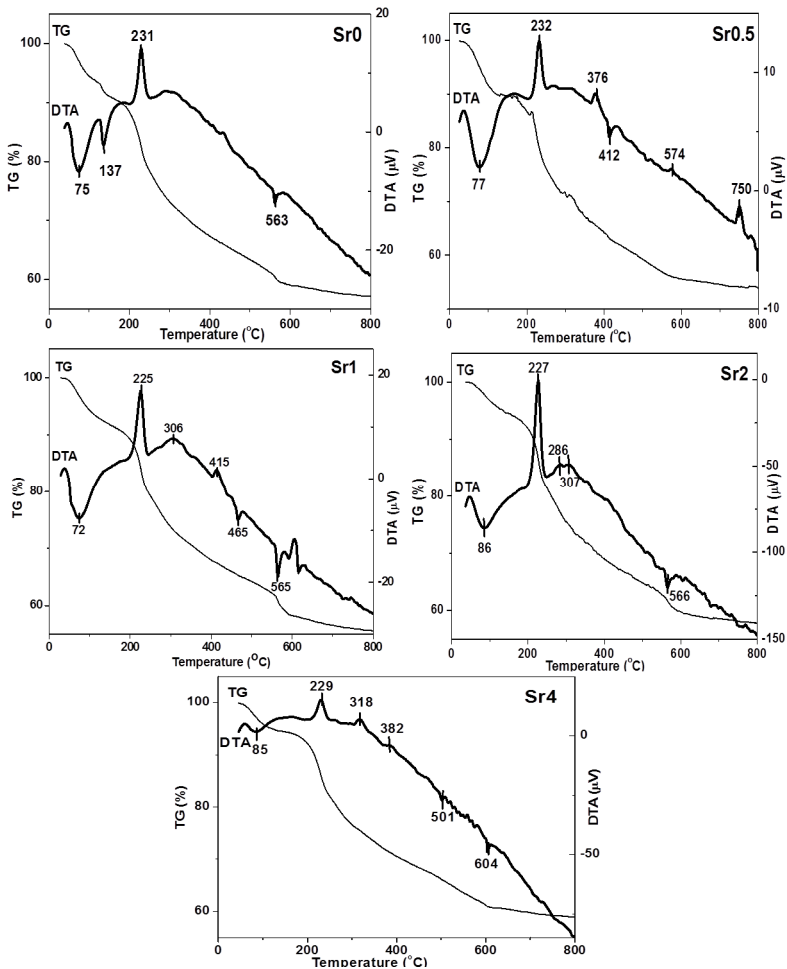


**Figure 1.** The DTA and TGA curves for xerogel samples dried at  $110\text{ }^{\circ}\text{C}$ .

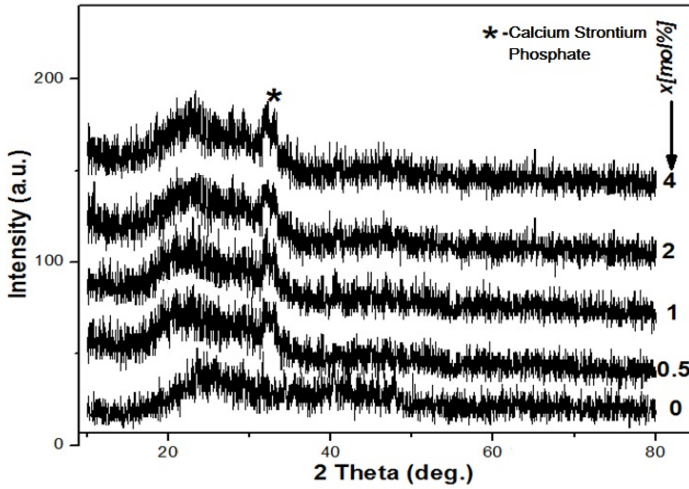


Figure 2. XRD patterns of  $65\text{SiO}_2 \cdot 5\text{P}_2\text{O}_5 \cdot (30-x)\text{CaO} \cdot x\text{SrO}$  glass samples.

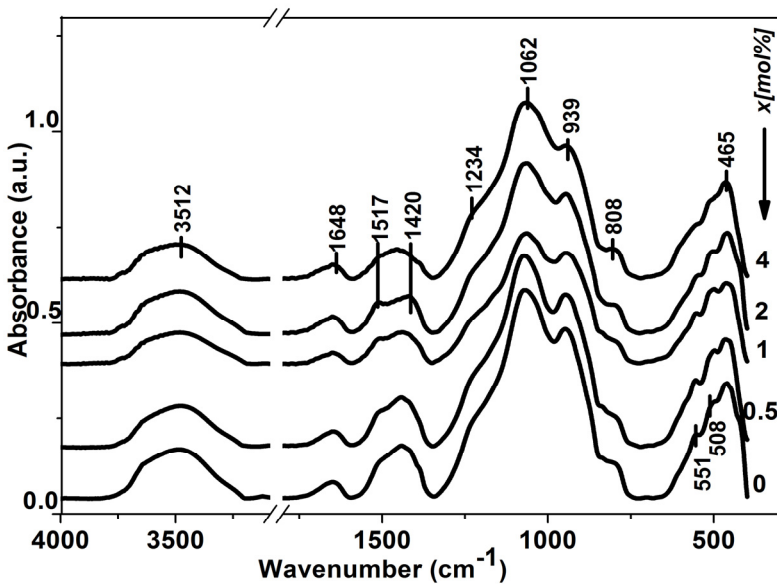
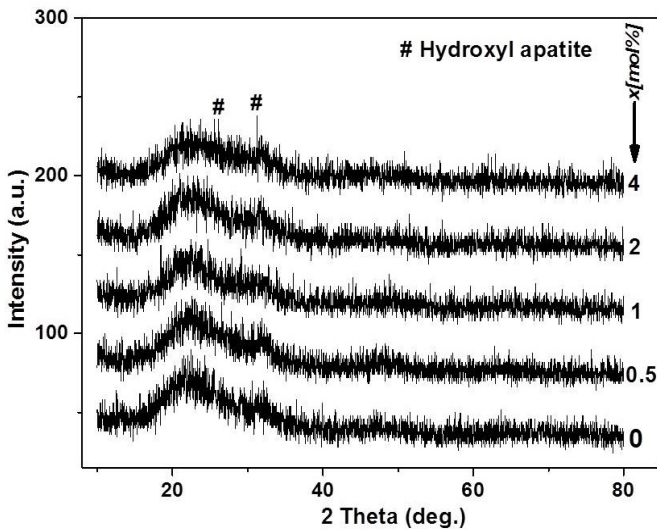


Figure 3. FT-IR spectra of  $65\text{SiO}_2 \cdot 5\text{P}_2\text{O}_5 \cdot (30-x)\text{CaO} \cdot x\text{SrO}$  glasses treated at  $600\text{ }^\circ\text{C}$ .

The bioactivity of the glasses was evaluated by soaking the samples during 14 days in SBF solution and characterizing them by XRD and FTIR techniques.

The XRD patterns for the immersed samples indicate the formation of a crystalline layer on the surface of the glasses (Figure 4), being observed one peak well developed at value  $2\theta=32.2^\circ$  which corresponds to the formation of hydroxyapatite (HA) crystals. This characteristic peak of apatite is observed in all specimens having lower peak intensity with the increase of strontium amount. It can be observed that for all the Sr concentrations, the glasses still indicate a good bioactivity.



**Figure 4.** XRD patterns of  $65\text{SiO}_2 \cdot 5\text{P}_2\text{O}_5 \cdot (30-x)\text{CaO} \cdot x\text{SrO}$  samples after immersion in SBF for 14 days.

FTIR spectra of all glasses show few changes after immersion in SBF (Figure 5) in comparison with the spectra before immersion.

All the spectra clearly show as the non-bridging oxygen Si-O band situated at  $920\text{ cm}^{-1}$  decreased in intensity after immersion. The band from  $790\text{ cm}^{-1}$  appeared in the spectra after immersion being assigned to Si-O-Si between the two adjacent silicates tetrahedra [30-32] which is an indicator for the formation of a silica gel layer. Furthermore, the band situated at  $878\text{ cm}^{-1}$  appeared in all the glasses and might correspond to the formation of complex carbonate species connected with the presence of  $\text{Ca}^{2+}$  ions on the surface [33]. Very clear changes can be seen in the region  $520\text{--}620\text{ cm}^{-1}$ , being the characteristic area for apatite. The doublet observed at  $567$  and  $614\text{ cm}^{-1}$  in all the investigated glasses corresponds to P-O bending vibrations in a  $\text{PO}_4^{3-}$  tetrahedron in hydroxyapatite [33] and denotes the glasses bioactivity.

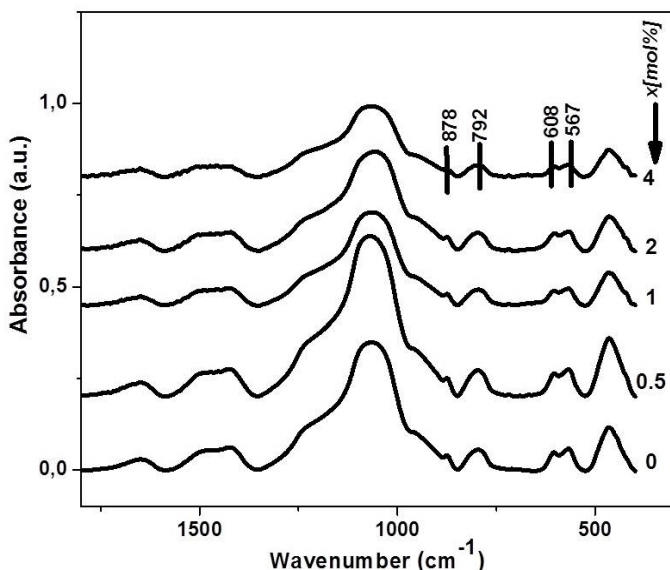


**Figure 5.** FTIR spectra of  $65\text{SiO}_2\cdot 5\text{P}_2\text{O}_5\cdot (30-x)\text{CaO}\cdot x\text{SrO}$  glasses after immersion in SBF for 14 days.

## CONCLUSIONS

Bioactive glasses based on  $\text{SiO}_2\text{-CaO-SrO-P}_2\text{O}_5$  system were obtained by sol-gel method. The structure of the samples thermally stabilized at  $600\text{ }^\circ\text{C}$  has a predominant amorphous character. The substitution of CaO with SrO up to 4 mol % does not inhibit the samples bioactivity, but the progressive increase of SrO content leads to the decrease of the absorption band assigned to the bioactive self-assembling hydroxyapatite layer. The samples can be considered for further investigation with respect to their bioactivity required for biomaterials used as scaffolds in bone tissue regeneration.

## EXPERIMENTAL SECTION

Samples of  $65\text{SiO}_2\cdot 5\text{P}_2\text{O}_5\cdot (30-x)\text{CaO}\cdot x\text{SrO}$  bioactive glass system ( $x = 0, 0.5, 1, \text{ and } 4$  mol%) were prepared following the sol-gel route. The precursors of  $\text{SiO}_2$ ,  $\text{P}_2\text{O}_5$ , CaO and SrO used for the synthesis of the glasses were tetraethylorthosilicate (TEOS), triethylphosphate (TEP), calcium nitrate tetrahydrate and strontium nitrate, respectively. All reagents were of analytical grade purity. In the first stage TEOS was mixed with  $\text{HNO}_3$  aqueous solution

having molar ratios  $\text{TEOS:H}_2\text{O:HNO}_3=1:9:0.1$  and stirred for 1h, then was added TEP and the stirring was continued for more 1h. In the second stage both strontium and calcium nitrates were dissolved in water. Finally the solutions were mixed together under continuous stirring for 1 h for the completion of hydrolysis reaction. The obtained sols were left 7 days at 37 °C for gelation and maturation, then the samples were dried for 24 h at 110 °C, and thermally treated at 600 °C for 2 h.

### **Differential thermal analysis and thermogravimetric analysis**

DTA/TG analysis were performed on Shimadzu type derivatograph DTG-60H SHIMADZU equipment, with a heating rates of 10 °C/min using alumina open crucibles, in order to investigate the thermal behavior of the dried sample.

### **X-ray diffraction**

The 600 °C treated samples were analyzed using an X-ray Shimadzu XRD-6000 diffractometer with a monochromator of graphite for  $\text{CuK}\alpha$  radiation ( $\lambda=1.5418\text{\AA}$ ) with Ni-filter. The diffractograms were recorded in  $2\theta$  range from 10° to 80° with a speed of 2°/min. The operation voltage and current were 40kV and 30mA, respectively.

### **FT-IR spectroscopy**

The FT-IR spectra were recorded at room temperature in the 400-4000  $\text{cm}^{-1}$  spectral range in absorbance mode with a JASCO FT/IR-6200 spectrometer, with an instrumental resolution of 4  $\text{cm}^{-1}$ . An amount of 2 mg of powder sample was thoroughly mixed with 200 mg of KBr and compressed to form pellets.

### **Assessment of the bioactivity**

Hydroxyapatite forming ability of the bioactive glasses was studied by immersing the samples in simulated body fluid (SBF) that has the ion concentrations and pH nearly equal to that of human blood plasma [34]. The samples immersed in SBF were kept in an oven at 37 °C for 14 days. The weight of glass per volume of SBF was 10 mg/ml for each sample. After 14 days the powders were filtrated, rinsed several times with distillate water and dried at room temperature.

### **ACKNOWLEDGMENTS**

The author R. Veres wishes to thank for the financial support of the Sectorial Operational Program for Human Resources Development 2007-2013, co-financed by the European Social Fund, under the project number POSDRU/159/1.5/S/132400 with the title „Young successful researchers – professional development in an international and interdisciplinary environment”.

## REFERENCES

1. Osteoporosis Prevention, Diagnosis, and Therapy, *National Institutes of Health Consensus Statement*, **2000**, March 27-29; *17*, 1.
2. Y.C. Fredholm, N. Karpukhina, D.S. Brauer, J.R. Jones, R.V. Law, R.G. Hill, *Journal of the Royal Society*, **2012**, *7*, 880.
3. L.L. Hench, R.J. Splinter, W. C. Allen, T. K.Greenlee, *Journal Biomedical Materials Research Symposium*, **1971**, *2*, 117.
4. L.L. Hench, H.A. Paschall, *Journal of Biomedical Materials Research*, **1973**, *7*, 25.
5. P.J. Marie, P. Ammann, G. Boivin, C. Rey, *Calcified Tissue International*, **2001**, *69*, 121.
6. P. J. Marie, *Current opinion in pharmacology*, **2005**, *5*, 633.
7. V. Timar, R. Ciceo-Lucacel, O. Hulpus, I. Ardelean, *Modern Physics Letters B* **2009**, *23*, 747.
8. K. Magyari, R. Stefan, D.C. Vodnar, A. Vulpoi, L. Baia, *Journal of Non-Crystalline Solids*, **2014**, *402*, 182.
9. P.I. Riti, A. Vulpoi, O. Ponta, V. Simon, *Ceramics International*, **2014**, *40*, Part B, 14741.
10. R. Ciceo Lucacel, O. Ponta, V. Simon, *Journal of Non-Crystalline Solids*, **2012**, *358*, 2803.
11. R. Veres, E. Vanea, C. Gruian, L. Baia, V. Simon, *Composites: Part B*, **2014**, *66*, 83.
12. M.D. O'Donnell, R. G. Hill, *Acta Biomaterialia*, **2010**, *6*, 2382.
13. G. Boivin, P. Deloffre, B. Prarat, G. Panezer, M. Boudeull, Y. Mauras, P. Allain, Y. Tsouderos, P.J. Meunier, *Journal of Bone and Mineral Research*, **1996**, *11*, 1302.
14. J.R. Jones, E. Gentleman, J. Polak, *Elements*, **2007**, *3*, 393.
15. S. Hesaraki, M. Gholami, S. Vazehrad, S. Shahrabi, *Materials Science and Engineering*, **2009**, *30*, 383.
16. E. Gentleman, Y.C. Fredholm, G. Jell, N. Lotfibakhshaiesh, M.D. O'Donnell, R.G. Hill, M.M. Stevens, *Biomaterials*, **2010**, *31*, 3949.
17. Y. Fredholm, N. Karpukhina, R.V. Law, R.G. Hill, *Journal of Non-Crystalline Solids*, **2010**, *356*, 2546.
18. A. Merolli, P.T. Leali, P.L. Guidi, C. Gabbi, *Journal of Materials Science: Materials in Medicine*, **2000**, *11*, 219.
19. Y. Fredholm, M.M. Stevens, R. Hill, *Proceedings of the 8th World Biomaterials Congress 28 May-1 June 2008*, Amsterdam RAI.
20. L. Lefebvre, J. Chevalier, L. Gremillard, R. Zenati, G. Thollet, D. Bernache Assolant, A. Govin, *Acta Materialia*, **2007**, *55*, 3305.
21. S. Jehabi, H. Oudadesse, J. Elleuch, S. Tounsi, H. Keskes, P. Pellen, T. Rehai, A. El Feki, H. El Feki, *Journal of the Korean Society for Applied Biological Chemistry*, **2013**, *56*, 533.



22. M.D. O'Donnell, P.L. Candarlioglu, C.A. Miller, E. Gentleman, M.M. Stevens, *Journal of Materials Chemistry*, **2010**, *20*, 8934.
23. M. Sitarz, M. Handke, W. Mozgawa, *Spectrochimica Acta Part A*, **2000**, *56*, 1819.
24. V. Aina, G. Malavasi, A. Fiorio Pla, L. Munaron, C. Morterra, *Acta Biomaterialia*, **2009**, *5*, 1211.
25. K. Omori, *Am Mineral*, **1971**, *56*, 1607.
26. A. Aronne, *Journal of Non-Crystalline Solids*, **2005**, *351*, 3610.
27. C. Chen, D. Huang, W. Zhu, X. Yao, *Applied Surfaces Science*, **2006**, *252*, 7585.
28. R. Veres, C. Ciuce, V. Simon, *Studia UBB Chemia*, **2011**, *3*, 193.
29. Z. Hong, R.L. Reis and J.F. Mano, *Journal of Biomedical Materials Research Part A*, **2009**, *88*, 304.
30. D.S. Brauer, N. Karpukhina, M.D. O'Donnell, R.V. Law, R.G. Hill, *Acta Biomaterialia*, **2010**, *6*, 3275.
31. C.Y. Kim, A.E. Clark, L.L. Hench, *Journal of Non-Crystalline Solids*, **1989**, *113*, 195.
32. X. Chen, X. Chen, D.S. Brauer, R.M. Wilson, R.G. Hill, N. Karpukhina, *Materials*, **2014**, *7*, 5470.
33. A. Goel, R.R. Rajagopal, J.M.F. Ferreira, *Acta Biomaterialia*, **2011**, *7*, 4071.
34. T. Kokubo, H. Kushitani, S. Sakka, T. Kitsugi, T. Yamamuro, *Journal of Biomedical Materials Research*, **1990**, *24*, 721.

